Energy Conversion and Management 65 (2013) 351–356

Contents lists available at SciVerse ScienceDirect

Energy Conversion and Management

journal homepage: www.elsevier.com/locate/enconman

Comparison of different modeling approaches for thermoelectric elements

G. Fraisse [a,*], J. Ramousse [a], D. Sgorlon [a], C. Goupil [b]

[a] Laboratoire Optimisation de la Conception et Ingénierie de l'Environnement, LOCIE-CNRS, UMR 5271, Polytech'Annecy-Chambéry, Savoie Technolac, 73376 Le Bourget-Du-Lac, France
[b] Laboratoire de Cristallographie et de Science des Matériaux, CRISMAT ENSICAEN, 6 Bd. Maréchal Juin, 14050 Caen, France

ARTICLE INFO

Article history:
Received 8 February 2012
Received in revised form 28 August 2012
Accepted 29 August 2012
Available online 17 October 2012

Keywords:
Modeling
Thermoelectric elements
Cooling
Power generation
Seebeck coefficient
Thomson effect

ABSTRACT

Simplified models are usually used to describe the behavior of thermoelectric elements due to their low computational effort needed for solving the physical behavior in a wide number of situations (e.g., in both heating/cooling mode – TEH or TEC – and in power generation mode – TEG). The accuracy of these models depends on different assumptions like: (i) the Thomson effect is assumed to be negligible and (ii) the thermoelectric properties are assumed to be constant in the thermoelectric leg and are estimated from the mean temperature of its two sides.

This paper attempts to analyze simplified models' accuracy, with regards to the performance (COP, efficiency), the voltage–current characteristics and the thermal/electrical power. The simplified models are compared to more accurate models, such as models based on an electrical analogy and on the finite element method (FEM). The benefits and drawbacks of each kind of model are discussed in order to help select the appropriate approach depending of the goal aimed. The improved simplified model using two different Seebeck coefficients with a constant Thomson coefficient greatly increases the accuracy of the results, particularly in TEG mode with large temperature differences between the two sides. The model based on the electrical analogy gives an intermediate approach between simplified models and FEM models. For one-dimensional modeling, the analogical model gives strictly the same results as those obtained with ANSYS (FEM-based software). In all the cases, we show that the key point is to use a null Thomson coefficient when a constant Seebeck coefficient is defined.

© 2012 Elsevier Ltd. All rights reserved.

1. Introduction

Thermoelectric effects were discovered during the first half of the 19th century. The Seebeck effect, highlighted in 1821 [1], implies that a voltage difference is created in the presence of a temperature difference between two different metals or semiconductors. A complementary effect, called the Peltier effect (1834) [2], results in a heat source or heat sink driven by an electrical current flowing through the junction between two different materials. Finally, the Thomson effect (1854) [3] reflects the heat released or absorbed when a single material is crossed by an electrical current and submitted to a thermal gradient. Although the physical phenomena are well known, the literature shows that they are sometimes not properly considered.

Although commercial softwares based on the finite element method (FEM) are able to model thermoelectric devices accurately, reliable simplified models are needed, both in electrical generator mode (TEG) and in heating/cooling pump mode (TEH or TEC). Two cases can illustrate this point:

- Long simulation periods: such simulations are needed when the electrical production or the heating/cooling coefficient of performance of thermoelectric devices has to be evaluated for several months (winter or summer, for example).
- Complex systems where the overall system is a combination of subsystems driven by different kind of energies. It is the case of a thermoelectric heat pump, for instance, coupled with a building (envelope, external surroundings, etc.) and other systems (radiator, heat exchanger, control devices, etc.).

In order to improve the modeling of thermoelectric devices, this paper focuses on the key part which is the thermoelectric leg. Different studies [4,5] highlight the importance of the Thomson effect when considering a TEC or TEG mode. Temperature dependence of the thermoelectric coefficients [6–10] has also been reported to be properly modeled, particularly in TEG mode where the temperature gradient in the material is large. This paper proposes to compare the accuracy of different simplified models with more accurate models. Two strategies are considered: (a) incorporating the Thomson effect and (b) considering the temperature dependence of the thermoelectric coefficients by distinguishing the volume effects (conduction, Joule, and Thomson effects) from the interface effects (Seebeck and Peltier). The last point was proposed by Jincan [11–13].

* Corresponding author.
E-mail addresses: gilles.fraisse@univ-savoie.fr (G. Fraisse), christophe.goupil@ensicaen.fr (C. Goupil).

0196-8904/$ - see front matter © 2012 Elsevier Ltd. All rights reserved.
http://dx.doi.org/10.1016/j.enconman.2012.08.022

Nomenclature

A	semiconductor (leg) section (m^2)
C	thermal capacitance ($J\,K^{-1}$)
COP	coefficient of performance (–)
Cp	specific heat at constant pressure ($J\,kg^{-1}\,K^{-1}$)
I	electrical current (A)
k	thermal conductivity ($W\,m^{-1}\,K^{-1}$)
K	thermal conductance ($W\,K^{-1}$)
L	semiconductor (leg) length (m)
P	electrical power (W)
Q	heat flux (W)
R	electrical resistance (Ω)
T	temperature (K)
ΔT	temperature difference between the two sides (K)
ZT	figure of merit (–)

Greek symbols

α	Seebeck coefficient ($V\,K^{-1}$)
η	electrical production efficiency (–)
ρ	density ($kg\,m^{-3}$)
σ	electrical conductivity ($\Omega^{-1}\,m^{-1}$)
τ	Thomson coefficient ($V\,K^{-1}$)

Subscripts

C	cold side
F	Fourier law (heat conduction)
H	hot side
T	Thomson effect

2. Thermoelectric models

Four major kinds of models are considered and compared in this paper:

- Standard simplified models, currently used in the literature [14–21]. An improved version of the simplified model (including the Thomson effect and a better evaluation of the thermoelectric coefficients as a function of temperature) is also studied in this paper [11–13].
- Analytical models giving the temperature and heat flux distributions in the materials [22].
- A model based on the electrical analogy between heat transfer and electricity [4].
- Numerical models based on the FEM [23–25].

The last two approaches can be used in transient mode by considering the semiconductor's thermal inertia. Fig. 1 represents the heat flux convention for the simplified models in cooling mode.

2.1. Global modeling: simplified models

The first way to model the thermoelectric elements is to use simplified models, which are based on a global balance of heat transfer and thermoelectric effects (macro approach).

2.1.1. Standard simplified model

The simplest approach to model a thermoelectric element is to set up an overall thermal balance, assuming a symmetrical distribution of the Joule effect between the hot and cold sides of the element. This assumption is commonly used to describe thermoelectric elements in both TEC/TEH mode [19,21,26–28] and TEG mode [15–18,29–33].

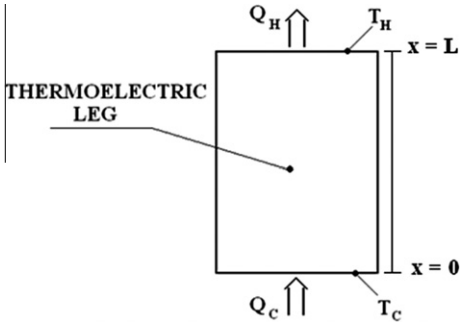

Fig. 1. Heat flux convention in a thermoelectric leg.

The Seebeck coefficient $\bar{\alpha}$, the thermal conductivity $\bar{k}$, and the electrical conductivity $\bar{\sigma}$ of the thermoelectric element are kept constant in the material and estimated from the mean temperature $\overline{T}$ of the hot and cold sides at T_H and T_C, respectively.

$$\overline{T} = \frac{T_H + T_C}{2}$$

This assumption is quite reliable in steady state as long as the Joule effect is not predominant. Other definitions can be considered from an evaluation of the temperature variation within the leg. It would allow calculating more precisely the average temperature. Nevertheless, the temperature variation is not *a priori* known.

Based on these assumptions, global energy balance in the whole leg produces the following expressions for the heat fluxes on the hot and cold sides, in TEC/TEH and TEG:

TEC/TEH:

$$Q_H = \overline{\alpha}\cdot I\cdot T_H - \overline{K}\cdot\Delta T + \frac{1}{2}\cdot\overline{R}\cdot I^2 \quad (1)$$

$$Q_C = \overline{\alpha}\cdot I\cdot T_C - \overline{K}\cdot\Delta T - \frac{1}{2}\cdot\overline{R}\cdot I^2 \quad (2)$$

TEG:

$$Q_H = \overline{\alpha}\cdot I\cdot T_H + \overline{K}\cdot\Delta T - \frac{1}{2}\cdot\overline{R}\cdot I^2 \quad (3)$$

$$Q_C = \overline{\alpha}\cdot I\cdot T_C + \overline{K}\cdot\Delta T + \frac{1}{2}\cdot\overline{R}\cdot I^2 \quad (4)$$

with

$$\overline{R} = \frac{L}{\overline{\sigma}\cdot A} \quad : \quad \text{electrical resistance} \quad (5)$$

$$\overline{K} = \frac{\overline{k}\cdot A}{L} \quad : \quad \text{thermal conductance} \quad (6)$$

The electrical power is the difference between the hot and cold thermal fluxes:

$$P = Q_H - Q_C \quad (7)$$

This leads to:

$$P = \overline{\alpha}\cdot I\cdot\Delta T + \overline{R}\cdot I^2 \,(\text{TEC/TEH}) \quad (8)$$

and

$$P = \overline{\alpha}\cdot I\cdot\Delta T - \overline{R}\cdot I^2 \,(\text{TEG}) \quad (9)$$

In TEC and TEH modes, the coefficient of performance (COP) is respectively given by:

$$COP_C = \frac{Q_C}{P} \quad COP_H = \frac{Q_H}{P} \tag{10}$$

and in TEG mode, the electrical efficiency is:

$$\eta = \frac{P}{Q_H} \tag{11}$$

In the above equations, the Thomson effect is null as the Seebeck coefficient is assumed constant (see Eq. (26)). Nevertheless, some papers show that the Thomson effect has to be correctly considered when its contribution is not negligible [34,35].

2.1.2. Improved simplified model [11–13]

Compared to the standard simplified model, the Thomson effect is taken into account and assumed to be equitably distributed on both sides of the semiconductor. This assumption has been validated in TEC mode [4]. A notable improvement in the accuracy of the model has been reported.

The second improvement proposed in [13] is relative to the evaluation of the thermoelectric coefficients as a function of temperature. The temperature used to evaluate each coefficient is defined by distinguishing the volume phenomena in the leg (conduction, Joule and Thomson effects) and the Seebeck effect taking place at the junction of two semiconductors. Thus the mean temperature $\bar{T}$ is used to evaluate the coefficients $\bar{k}, \bar{\sigma}$, and $\bar{\tau}$. Regarding the Seebeck effect, the temperature of each side is used to determine α_C and α_H at T_C and T_H, respectively.

The thermal fluxes are thus expressed as:

TEC/TEH:

$$Q_H = \alpha_H \cdot I \cdot T_H - \overline{K} \cdot \Delta T + \frac{1}{2} \cdot \overline{R} \cdot I^2 - \frac{1}{2} \cdot \overline{\tau} \cdot I \cdot \Delta T \tag{12}$$

$$Q_C = \alpha_C \cdot I \cdot T_C - \overline{K} \cdot \Delta T - \frac{1}{2} \cdot \overline{R} \cdot I^2 + \frac{1}{2} \cdot \overline{\tau} \cdot I \cdot \Delta T \tag{13}$$

From the expression of the electrical power (Eq. (7)):

$$P = (\alpha_H \cdot T_H - \alpha_C \cdot T_C) \cdot I + \overline{R} \cdot I^2 - \overline{\tau} \cdot I \cdot \Delta T \tag{14}$$

Eqs. (12) and (13) show that the Thomson effect tends to counter the Joule effect (if $\bar{\tau} > 0$ and $I > 0$). Consequently, the Thomson effect is advantageous in cooling mode, whereas it is disadvantageous in heating mode.

For TEC/TEH modes, if the temperature difference ΔT is low, the Seebeck coefficients and α_H can be replaced by $\bar{\alpha}$, giving:

$$P \approx (\bar{\alpha} - \bar{\tau}) \cdot I \cdot \Delta T + \overline{R} \cdot I^2 \tag{15}$$

TEG:

$$Q_H = \alpha_H \cdot I \cdot T_H + \overline{K} \cdot \Delta T - \frac{1}{2} \cdot \overline{R} \cdot I^2 - \frac{1}{2} \cdot \overline{\tau} \cdot I \cdot \Delta T \tag{16}$$

$$Q_C = \alpha_C \cdot I \cdot T_C + \overline{K} \cdot \Delta T + \frac{1}{2} \cdot \overline{R} \cdot I^2 + \frac{1}{2} \cdot \overline{\tau} \cdot I \cdot \Delta T \tag{17}$$

The electrical power is thus:

$$P = (\alpha_H \cdot T_H - \alpha_C \cdot T_C) \cdot I - \overline{R} \cdot I^2 - \overline{\tau} \cdot I \cdot \Delta T \tag{18}$$

In this case, the Thomson effect is disadvantageous (if $\bar{\tau} > 0$ and $I > 0$), since it contributes to decrease the efficiency.

If ΔT is low (this is generally not true, except in the case of thermoelectric microgeneration [36]), $\alpha_C \approx H$ and can be replaced by $\bar{\alpha}$ estimated at $\bar{T}$, giving:

$$P \approx (\overline{\alpha} - \overline{\tau}) \cdot I \cdot \Delta T - \overline{R} \cdot I^2 \tag{19}$$

2.2. Model derived from the local energy balance

More complex models are used to describe the thermoelectric element behavior more precisely. They are based on a local energy balance, detailed in the following.

In transient regime, the local energy balance in the leg N is written [22,37]:

$$\rho \cdot Cp \cdot \frac{\partial T(x,t)}{\partial t} = k \cdot \frac{\partial}{\partial x}\left(\frac{\partial T(x,t)}{\partial x}\right) + \frac{1}{\sigma} \cdot \left(\frac{I}{A}\right)^2 - \tau \cdot \frac{I}{A} \cdot \frac{\partial T(x,t)}{\partial x} \tag{20}$$

At both leg extremities (at $x = 0, T = T_C$ and at, $T = T_H$), the boundary conditions have to include the heat source/sink related to the Seebeck effect:

$$Q(x=0,t) = \alpha \cdot I \cdot T_C - k \cdot A \cdot \left.\frac{\partial T}{\partial x}\right|_{(x=0,t)}$$

$$Q(x=L,t) = \alpha \cdot I \cdot T_H - k \cdot A \cdot \left.\frac{\partial T}{\partial x}\right|_{(x=L,t)} \tag{21}$$

2.2.1. Analytical model

In steady state, when the thermoelectric coefficients and the leg section are assumed constant along the leg length, the analytical solution of the heat flux and the temperature can be derived from the above equations, including the Thomson effect [22]. In TEC mode, this gives:

$$Q(x) = \overline{\alpha} \cdot I \cdot T(x) - \frac{\overline{k} \cdot I}{\overline{\tau} \cdot \overline{\sigma}} + \frac{\left(-Q_F + \frac{\overline{k} \cdot I}{\overline{\sigma} \cdot \overline{\tau}}\right) \cdot \frac{Q_T}{Q_F}}{\exp\left[\frac{Q_T}{Q_F}\left(1 - \frac{x}{L}\right)\right] - \exp\left[-\frac{Q_T}{Q_F}\frac{x}{L}\right]} \tag{22}$$

$$T(x) = T_C + (T_H - T_C - \frac{c}{b}L) \cdot \frac{\exp(-b \cdot x) - 1}{\exp(-b \cdot L) - 1} + \frac{c}{b}x \tag{23}$$

With $b = -\frac{\overline{\tau} \cdot I}{\overline{k} \cdot A}$ and $c = -\frac{I}{\overline{k} \cdot \overline{\sigma} \cdot A}$ $Q_F = \overline{k} \cdot A \cdot \frac{\Delta T}{L}$ (conduction flux, Fourier) and $Q_T = \overline{\tau} \cdot I \cdot \Delta T$ (Thomson).

2.2.2. Electrical analogy model

The electrical analogy [38] helps to model complex phenomena easily such as the thermal dependence of the thermoelectric coefficients, transient regime, or variable section of the thermoelectric leg. This approach, derived from Eq. (20), is presented in [4]. In order to take into account all the thermoelectric effects (Peltier, Joule, and Thomson) and their dependence on temperature, the leg is discretized in N nodes (Fig. 2).

In steady state, the discretization of the balance equation (Eq. (20)) at each node n (from 1 to N) gives:

$$\frac{T_{n-1} - T_n}{\frac{1}{2} \cdot \left(\frac{1}{K_{n-1}} + \frac{1}{K_n}\right)} + \frac{T_{n+1} - T_n}{\frac{1}{2} \cdot \left(\frac{1}{K_{n+1}} + \frac{1}{K_n}\right)} + \Phi_n = 0 \tag{24}$$

In order to respect the local energy balance, the heat flux Φ_n to add at each node in the electrical analogy is given by:

$$\Phi_n = R_n \cdot I^2 - \tau_n \cdot I \cdot \frac{T_{n+1} - T_{n-1}}{2} \tag{25}$$

The same boundary conditions as above (Eq. (21)) are imposed. In each element, the thermal conductance K_n and the electrical resistance R_n are estimated with respect to the local temperature and the leg section (A_n can vary in this model). It means that all the thermal and thermo-electrical parameters are evaluated at the temperature of each node.

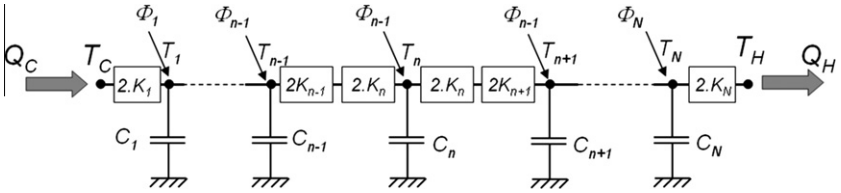

Fig. 2. Analogical scheme of the thermoelectric phenomena with the thermal capacitances $C_n = \rho_n \cdot Cp_n \cdot \frac{L}{N} \cdot A$ and thermal conductances $K_n = \frac{k_n \cdot A}{L/N}$.

2.2.3. Numerical models based on FEM software

The nonlinearity in thermoelectric material modeling resulting from the temperature dependency of material properties requires in most cases to use available computational techniques such as FEM software. The model is implemented using the ANSYS program (version 12.1), in which dedicated numerical heat transfer schemes of thermoelectricity are implemented. The equations used in ANSYS are also derived from Eq. (20). In our study, a steady state analysis leads to the thermal and electric fields. The solution is obtained with the ANSYS Mechanical Solver based on the Newton–Raphson method. The main advantage of such FEM software is to allow the coupling of thermoelectric simulations to computational fluid dynamics models. This kind of approach is also suitable for 3D geometries and for transient regime.

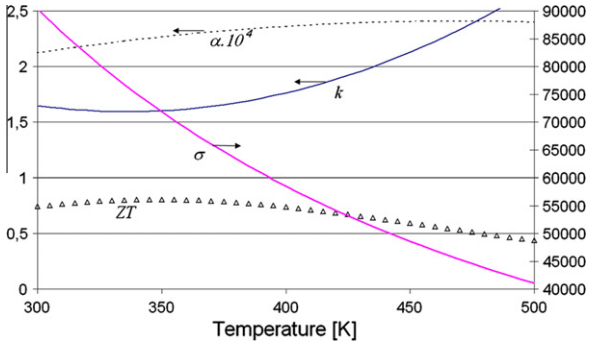

Fig. 3. Temperature dependences of α, σ, k and ZT.

3. Steady state comparison of the models

The comparative study is based on the well known Bismuth Telluride Bi_2Te_3 material. The geometric and thermoelectric data (quadratic polynomial [39]) are given in Table 1. Fig. 3 shows the temperature dependence of α, σ, k, and the figure of merit ZT. The value of ZT is 0.74 at the mean temperatures of 300 K and 400 K.

The numerical solution of the equations concerning the analogical model is obtained with the solver Engineering Equation Solver (EES). EES gives the numerical solution of a set of algebraic equations. It can also be used to solve differential and integral equations [40]. The steady-state model based on the finite element method (FEM), developed with ANSYS software, is considered as the reference for the following model comparison. Indeed, this model has been validated by experimental data from real thermoelectric devices [41]. In our study, all material properties are considered to be isotropic. A total of 19, 130 elements are used and the convergence criteria are set to 10^{-6} for heat transfer and 10^{-12} for voltage and current. A grid sensitivity analysis was performed for the ANSYS and electrical analogy model to check its grid independency. Concerning the ANSYS model, the default method for meshing was used (*Patch Conforming* and *Sweeping Method* with quadrilaters on top/bottom faces of the thermoelectric leg). The same refined grid was considered for both TEC and TEG configurations (70 layers in the leg length). For the electrical analogy model, 100 nodes were considered. The results were checked to vary slightly when the number of nodes exceeds 30 nodes. The different assumptions relative to the Seebeck and Thomson effects for each model are summarized in Table 2.

Table 1
Geometric and thermoelectric data (TEC mode).

Length	$L = 1.4 \times 10^{-3}$ m
Section	$A = 1.4 \times 10^{-6}$ m^2
Thermal conductivity	$k_{(T)} = (62605 - 277.7 * T + 0.4131 * T^2) \times 10^{-4}$ (W m^{-1} K^{-1})
Electrical conductivity	$\sigma_{(T)} = (5112 + 163.4 * T + 0.6279 * T^2)^{-1} \times 10^{10}$ (Ω^{-1} m^{-1})
Seebeck coefficient	$\alpha_{(T)} = (22224 + 930.6 * T - 0.9905 * T^2) \times 10^{-9}$ (V/K)
Thomson coefficient	$\tau_{(T)} = (930.6 - 0.9905 * T * 2) \times 10^{-9} * T$ (V/K)

Table 2
Assumptions relative to the Seebeck and Thomson coefficients for the different models.

Cases	Model	Seebeck	Thomson	Ref.
1	Simplified	$\bar{\alpha}$	0	[14–21]
2	Simplified (Thomson)	$\bar{\alpha}$	$\bar{\tau}$	
3	Simplified (improved)	$\alpha_C(T_C)$ and $\alpha_H(T_H)$	$\bar{\tau}$	[13]
4	Analytical	$\bar{\alpha}$	$\bar{\tau}$	[22]
5	Electrical analogy	$\alpha(T)$	$\tau(T)$	[4]
6		$\bar{\alpha}$	$\bar{\tau}$	
7		$\alpha(T)$	0	
8	ANSYS (FEM)	$\alpha(T)$	$T \cdot \frac{d\alpha(T)}{dT}$	[23,25]
9		$\bar{\alpha}$	0	

3.1. TEC mode

The hot and cold operating temperature are set to: $T_H = 300$ K (hot temperature at $x = 0$) and $T_C = 270$ K (cold temperature at $x = L$).

The coefficient of performance COP_C and cold thermal power Q_C versus electrical current are plotted in Fig. 4 for the different models considered. First, one can see that the results of the electrical analogy model (case 5; see Table 2) are identical to the results of the FEM model with case 8 (ANSYS) of Table 2. It can then be noted that the standard (case 1) and the improved simplified (case 3) models give identical results. It can be explained by the small temperature difference between the two sides, leading to low Thomson effect (it is not the case in TEG mode). The results for cases 1 and 3 are similar to the reference for currents lower than 4A regarding the COP_C and lower than 6A for the cold thermal power. Nevertheless, the maximum values of COP_C and Q_C can be evaluated precisely. The analytical solution (case 4) plotted in Fig. 4 gives the worst results compared to the reference (cases 8 and 5), although the Thomson effect is included. Indeed, the difference relative to the reference is 22% on the maximum COP_C and 8% on the

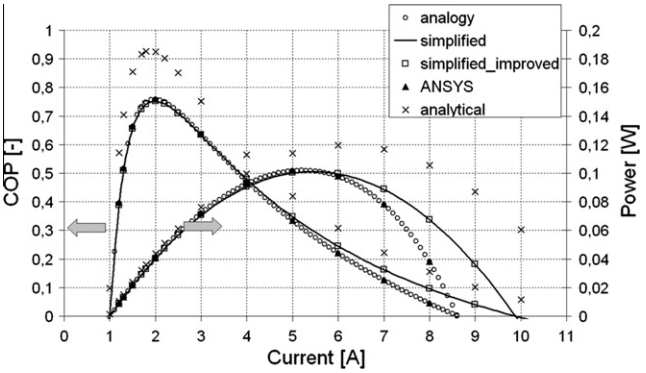

Fig. 4. Comparison of the COP_C and cold thermal power (TEC mode).

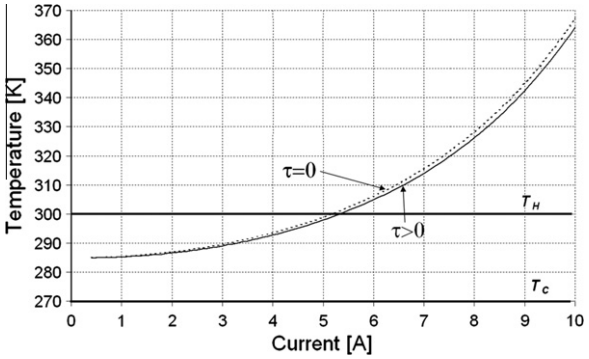

Fig. 5. Mean temperature (cases 5 and 7) vs. current, with and without the Thomson coefficient (T_H = 300 K and T_C = 270 K).

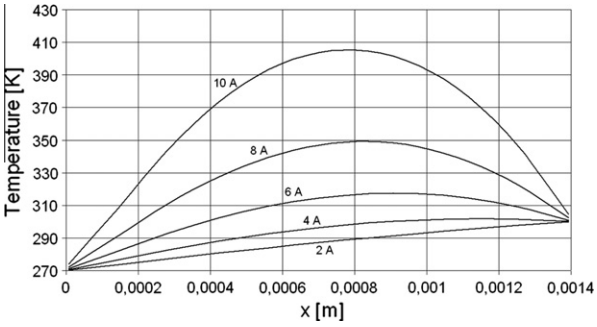

Fig. 6. Temperature variation within the leg (case 5).

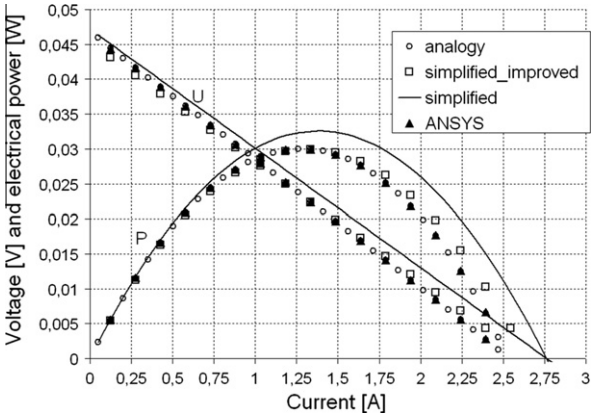

Fig. 7. Voltage and electrical power vs. current for the different models considered (T_H = 500 K and T_C = 300 K).

maximum Q_C. This can easily be explained by the Thomson coefficient expression:

$$\tau = T \cdot \frac{d\alpha}{dT} \tag{26}$$

This equation shows that the Thomson coefficient must not be used in cases of a constant Seebeck coefficient calculated with the mean temperature. As a confirmation, we checked that the electrical analogy model with constant coefficients (case 6) and the simplified model with the Thomson coefficient (case 2) give the same poor results as the analytical model (case 4).

The mean temperature of the leg (electrical analogy model, with (case 5) and without the Thomson effect (case 7)) are plotted vs. electrical current in Fig. 5. The mean temperature increases significantly as current increases and moves away from the average temperature of the cold and hot sides. This comes from the Joule effect increasing as current increases. This can explain that the standard (case 1) and the improved simplified (case 3) models give greater differences compared to the reference for currents greater than 6A regarding the cold thermal power. The temperature variation within the leg is illustrated in Fig. 6 (case 5), as a function of the electrical current. The figure clearly shows the limit to consider a mean temperature of the hot and cold side for the calculation of the physical properties.

Finally we observed that the maximal COP_C obtained with the analogy model without the Thomson effect (case 7) is 17% lower than the reference (cases 5 and 8), even if Fig. 5 shows that the temperature distribution in the leg is only slightly influenced by the Thomson effect (case 5 compared with case 7). The Thomson effect contribution can be highlighted only with the analogy model, because the Thomson coefficient is automatically estimated from the Seebeck coefficient in ANSYS software with Eq. (32). Consequently, the only valid way to set a zero Thomson coefficient in ANSYS software is to define a constant Seebeck coefficient (case 9).

3.2. TEG mode

The following operating conditions are considered for the TEG mode (the geometrical and thermoelectric data given in Table 1 remain valid): T_H = 500 K (hot temperature at $x = 0$) and T_C = 300 K (cold temperature at $x = L$).

In Fig. 7 is plotted the voltage and electrical power vs. current for the different models considered. The difference in maximal power between the standard simplified model (case 1) and the reference (case 8) is approximately 9%. However, the improved simplified model (case 3) gives the same value as the reference. In addition, for any electrical current, the error in voltage and efficiency induced by the standard simplified model (case 1) is greater than the errors in the improved simplified model. We also noted a slight divergence between the improved simplified model and the reference when current moves away from the optimal current, giving the maximum electrical power.

4. Conclusion

Different kinds of models were used and compared to simulate thermoelectric phenomena in a thermoelectric leg.

No significant difference between the standard and the improved simplified models appears in TEC and TEH modes. On the contrary, a notable overestimation of the maximum efficiency was noted with the standard simplified model in TEG mode. The improved simplified model shows a marked improvement

compared to the standard simplified model, because the Seebeck coefficients are determined at the hot and cold sides (the other coefficients were estimated at the average temperature of the sides) and the Thomson coefficient is calculated as a function of the mean temperature.

Considering a constant Seebeck coefficient intrinsically means a zero Thomson coefficient. For any model, the Thomson coefficient must not be taken into account when the Seebeck coefficient is assumed to be constant. This is the reason why the analytical model appears to be the less accurate. In any case we observe that the introduction of the Thomson contribution as an additive term is only valid if a thermal dependence of the value of the Seebeck coefficient is considered. It should be noticed that the electrical analogy model is very efficient since it gives almost the same results as the FEM approach does, in a very practical and fast way.

Acknowledgments

This study is financed by CNRS in the framework of "*Programme Interdisciplinaire Energie du CNRS*" (OTOGEHT Project) and the "*Fonds Unique Interministériel*" (FUI, SysPACTE Project).

References

[1] TJ. Seebeck. Ueber den Magnetismus der galvanischen Kette. Abh Akad Wiss. Berlin; 1821. p. 289.
[2] Peltier JCA. Nouvelles expériences sur la caloricité des courants électriques. Ann. Chem. Phys 1834;371–56.
[3] Thomson W. Account of researches in thermo-electricity. Philos Mag 1854;5:62–8.
[4] Fraisse G, Goupil C, Lazard M, Serrat JY. Study of thermoelement's behaviour through a modeling based on electrical analogy. Int J Heat Mass Trans 2010;53(17–18):3503–12.
[5] Huang MJ, Yen RH, Wang AB. The influence of the Thomson effect on the performance of a thermoelectric cooler. Int J Heat Mass Trans 2005;48:413–8.
[6] Sunderland JE, Burak NT. The influence of the Thomson effect on the performance of a thermoelectric power generator. Solid-State Electr 1964;7(6):465–71. doi:10.1016/0038-1101(64)90044-9.
[7] Adamson WL. The effects of the Thomson coefficient and variable resistivity on thermoelectric heat pump performance. Master's thesis, Georgia Institute of Technology; 1965. <http://smartech.gatech.edu/handle/1853/19691>.
[8] Adamson WL, Sunderland JE. The influence of the Thomson coefficient and variable resistivity on thermoelectric heat pump performance. Solid-State Electr 1966;9(2):105–12. http://dx.doi.org/10.1016/0038-1101(66)90081-.
[9] Yamashita O. Effect of the temperature dependence of electrical resistivity on the cooling performance of a single thermoelectric element. Appl Energy 2008;85:1002–14.
[10] Yamashita O. Effect of linear and non-linear components in the temperature dependences of thermoelectric properties on the cooling performance. Appl Energy 2009;86:1746–56.
[11] Burshtein AI. An investigation of the steady-state heat flow through a current-carrying conductor. Sov Phys-Tech Phys 1957;2:1397–406.
[12] Moizhes BY. The influence of the temperature dependence of physical parameters on the efficiency of thermoelectric generators and refrigerators. Sov Phys – Solid State 1960;2:671–80 [Translated from Fizika Tverdogo Tela, 1960;2(4):728–37].
[13] Jincan C, Zijun Y. The influence of Thomson effect on the maximum power output and maximum efficiency of a thermoelectric generator. J Appl Phys 1996;79(11):8823–8.
[14] Ioffe AF. Semiconductor thermoelements and thermoelectric cooling. London: Infosearch, Ltd.; 1957.
[15] Chen L, Li J, Sun F, Wu C. Performance optimization of a two-stage semiconductor thermoelectric-generator. Appl Energy 2005;82:300–12.
[16] Chen L, Li J, Sun F, Wu C. Performance optimization of a two-stage thermoelectric heat-pump with internal and external irreversibilities. Appl Energy 2008;85:641–9.
[17] Hsiao YY, Chang WC, Chen SL. A mathematic model of thermoelectric module with applications on waste heat recovery from automobile engine. Energy 2010;35(3):1447–54.
[18] Khattab NM, El Shenawy ET. Optimal operation of thermoelectric cooler driven by solar thermoelectric generator. Energy Convers Manage 2006;47(4):407–26.
[19] Dai YJ, Wang RZ, Ni L. Experimental investigation and analysis on a thermoelectric refrigerator driven by solar cells. Solar Energy Mater Solar Cells 2003;77(4):377–91.
[20] Yu J, Zhao H. A numerical model for thermoelectric generator with the parallel-plate heat exchanger. J Power Sources 2007;172(1):428–34.
[21] Khire RA, Messac A, Van Dessel S. Design of thermoelectric heat pump unit for active building envelope systems. Int J Heat Mass Trans 2005;48(19–20):4028–40.
[22] Chakraborty A, Saha BB, Koyama S, Ng KC. Thermodynamic modelling of a solid state thermoelectric cooling device: temperature–entropy analysis. Int J Heat Mass Trans 2006;49(19–20):3547–54.
[23] Saber HH, El-Genk MS. A three-dimensional, performance model of segmented thermoelectric converters, using ANSYS commercial software. In: El-Genk MS, editor. Proceedings space technology and applications international forum (STAIF-02), AIP conference proceedings, New York: American Institute of Physics; 2002. p. 999.
[24] Antonova EE, Looman DC. Finite elements for thermoelectric device analysis in ANSYS. In: 24th International conference on thermoelectrics (ICT); 2005. p. 215–18.
[25] Madenci E, Guven I. The finite element method and applications in engineering using ANSYS. Springer; 2006. p. 686.
[26] Min G, Rowe DM. Cooling performance of integrated thermoelectric micro-cooler. Solid-State Electr 1999;43:923–9.
[27] Riffat SB, Ma X. Improving the coefficient of performance of thermoelectric cooling systems: a review. Int J Energy Res 2004;28:753–68.
[28] Xu X, Van Dessel S, Messac A. Study of the performance of thermoelectric modules for use in active building envelopes. Build Environ 2007;42(3):1489–502.
[29] Nuwayhid RY, Moukalled F, Noueihed N. On entropy generation in thermoelectric devices. Energy Convers Manage 2000;41:891–914.
[30] Nuwayhid RY, Shihadeh A, Ghaddar N. Development and testing of a domestic woodstove thermoelectric generator with natural convection cooling. Energy Convers Manage 2005;46(9–10):1631–43.
[31] Gou X, Xiao H, Yang S. Modeling, experimental study and optimization on low-temperature waste heat thermoelectric generator system. Appl Energy 2010;87(10):3131–6.
[32] Qiu K, Hayden ACS. Development of a thermoelectric self-powered residential heating system. J Power Sources 2008;180(2):884–9.
[33] Kousksou T, Bédécarrats JP, Champier D, Koch S, Brillet C, Pignolet P. Numerical analysis of thermoelectric power generation: aircraft systems application. In: International conference on efficiency, cost, optimization, simulation, and environmental impact of energy systems, ECOS; 2010. p. 8.
[34] Pramanick AK, Das PK. Constructal design of a thermoelectric device. Int J Heat Mass Trans 2006;49:1420–9.
[35] Gurevich YG, Logvinov GN. Theory of thermoelectric cooling in semiconductors structures. Revista mexicana de fisica 2007;53(5):337–49.
[36] Agbossou A, Zhang Q, Sebald G, Guyomar D. Solar micro-energy harvesting based on thermoelectric and latent heat effects. Part I: theoretical analysis. Sensors Actuators 2010;163:277–83.
[37] Xuan XC, Ng KC, Yap C, Chua HT. Optimization of two-stage thermoelectric coolers with two design configurations. Energy Convers Manage 2002;43(15):2041–52.
[38] Fraisse G, Viardot C, Lafabrie O, Achard G. Development of a simplified and accurate building model based on electrical analogy. Energy Build 2002;34(10):1017–31.
[39] Riffat SB, Ma X, Wilson R. Performance simulation and experimental testing of a novel thermoelectric heat pump system. Appl Thermal Eng 2006;26:494–501.
[40] EES manual, Engineering Equation Solver. V8, F-Chart Software. p. 313.
[41] Chen M, Rosendahl LA, Condra T. A three-dimensional numerical model of thermoelectric generators in fluid power systems. Int J Heat Mass Trans 2011(1–3):345–55.